The magnetic field in HD 161701, the only binary system identified to consist of an HgMn primary and an Ap secondary[★]

S. Hubrig,[1][†] T. A. Carroll,[1] J. F. González,[2] M. Schöller,[3] I. Ilyin,[1] C. Saffe,[2] F. Castelli,[4] F. Leone[5] and M. Giarrusso[5,6]

[1]*Leibniz-Institut für Astrophysik Potsdam (AIP), An der Sternwarte 16, D-14482 Potsdam, Germany*
[2]*Instituto de Ciencias Astronómicas, de la Tierra, y del Espacio (ICATE), 5400 San Juan, Argentina*
[3]*European Southern Observatory, Karl-Schwarzschild-Str. 2, D-85748 Garching, Germany*
[4]*Istituto Nazionale di Astrofisica, Osservatorio Astronomico di Trieste, via Tiepolo 11, I-34143 Trieste, Italy*
[5]*Dipartimento di Fisica e Astronomia, Sezione Astrofisica, Università di Catania, Via S. Sofia 78, I-95123 Catania, Italy*
[6]*INAF-Osservatorio Astrofisico di Catania, Via S. Sofia 78, I-95123 Catania, Italy*

ABSTRACT

Recently, we performed a complete study of the SB2 system HD 161701 with an orbital period of 12.5 d, consisting of an HgMn primary and a classical Ap secondary. Since this is the first system identified with this particular combination of peculiar stars, a study of the presence of a magnetic field in both components is of considerable interest to astronomers studying stellar magnetism and the impact of the presence of a magnetic field in binary systems. Apart from HD 161701, only one other close binary systems with a magnetic Ap component, the system HD 98088, is currently known. Using high accuracy radial velocity planet searcher (HARPS) polarimetric spectra obtained on six consecutive nights, we detect in the Ap component a mean longitudinal magnetic field of up to 200 G varying in strength over the orbital/rotational period. The magnetic field behaviour in this component is closely related to the position of the primary component, exhibiting negative polarity. There was no detection of any longitudinal magnetic field with an upper limit of ∼90 G in the primary.

Key words: stars: abundances – stars: atmospheres – stars: binaries: spectroscopic – stars: chemically peculiar – stars: individual: HD 161701 – stars: magnetic field.

1 INTRODUCTION

HD 161701 is a binary system formed by two chemically peculiar stars in an almost circular orbit with a 12.451 d period. The primary is a 4.0 $M_\odot$ star with a chemical pattern typical of HgMn stars with notable overabundances of P, Mn, Ga, Y, Xe, and Hg. The secondary is a 2.4 $M_\odot$ star, identified as a classical Ap star, with overabundances of 1–2 dex in Ti, Cr, Mn, and Fe, of 2–3 dex in Sr and Y, and 2.5–5 dex in all rare-Earth elements (REE; González et al. 2014). The orbital solution indicates a nearly circular orbit with an eccentricity $e = 0.0043$, only marginally different from zero, and projected rotational velocities $v \sin i = 16.8 \pm 0.6$ km s^{-1} for the primary and $v \sin i = 7.6 \pm 1.1$ km s^{-1} for the secondary. This implies that an efficient circularization and synchronization mechanism has been at work in this system. Furthermore, spectral lines of various elements in the spectra of both components show variability with the rotational/orbital period. In the HgMn primary, the spectral lines of Mn and Cr become stronger near the second quadrature ($\phi \approx 0.85$) than near the first quadrature ($\phi \approx 0.17$). As for the secondary component, the surface region permanently facing the primary star has the highest abundance of REE and Ti, while Fe is concentrated in the surface region hidden to the primary. For both components, the inhomogeneous surface element distribution appears to be clearly affected by the presence of the companion. González et al. (2014) suggest that large-scale magnetic fields of the components may account for such a high degree of circularization and synchronization reached in this system with a relatively long orbital period. However, no magnetic field measurements have been attempted so far for HD 161701. In this work, we report the results of our spectropolarimetric study of this system, which is the first system identified with this particular combination of peculiar stars.

2 OBSERVATIONS

Six spectra with a spectral resolution of 115 000 were obtained in the polarimetric configuration of high accuracy radial velocity planet

Table 1. Logbook of the HARPS observations.

| HJD	Phase	RV$_A$ (km s^{-1})	RV$_B$ (km s^{-1})	S/N$_{4400}$
245 6143.701	0.82	36.3	−111.6	150
245 6144.600	0.89	20.3	−84.4	145
245 6145.573	0.97	−5.6	−40.3	125
245 6146.620	0.05	−37.6	12.9	125
245 6147.644	0.13	−63.0	55.4	130
245 6148.630	0.21	−77.2	79.1	140
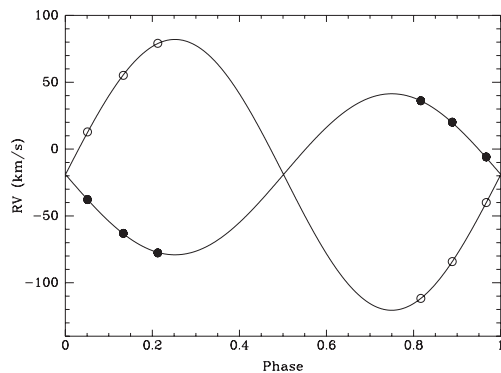
Figure 1. Radial velocity curves for the primary and the secondary. Filled circles correspond to the primary component while open circles correspond to the secondary component.

searcher (HARPS) over six consecutive nights covering a little less than half of the orbital period. The reduction was performed using the HARPS data reduction software available at the 3.6 m telescope in Chile. The normalization procedure of the HARPS spectra to the continuum level is described in detail in the work of Hubrig et al. (2013).

The observing logbook is presented in Table 1, where the first column gives the date of observation, and the second column the corresponding orbital/rotational phase calculated using the ephemeris HJD = 2453892.3112(12) + 12^d.451 23(4)E. The corresponding radial velocities (RVs) are listed in columns 3 and 4, followed by the signal-to-noise ratio (S/N) per resolution element of the spectra in the wavelength region around 4400 Å. The formal errors of the RVs account for ∼0.1 km s^{-1} for the primary and ∼0.2 km s^{-1} for the secondary. The observations are carried out in orbital phases from 0.82 to 0.21. In Fig. 1, we present the RV curves with the HARPS observations marked by filled circles for the primary and open circles for the secondary.

3 SPECTRAL VARIABILITY AND MAGNETIC FIELD MEASUREMENTS

Typically, an inhomogeneous chemical abundance distribution is observed only on the surface of upper-main-sequence stars with large-scale organized magnetic fields. The abundance distribution of certain elements in these stars is usually non-uniform and non-symmetric with respect to the rotation axis, but shows a kind of symmetry between the topology of the magnetic field and the element distribution. González et al. (2014) mention that the spectral lines of Mn and Cr in the spectra of the primary in HD 161701 become stronger near the second quadrature at $\phi \approx 0.85$ and weaker at the first quadrature at $\phi \approx 0.17$. To better understand the chemical spot pattern on the surface of the HgMn primary, we selected five
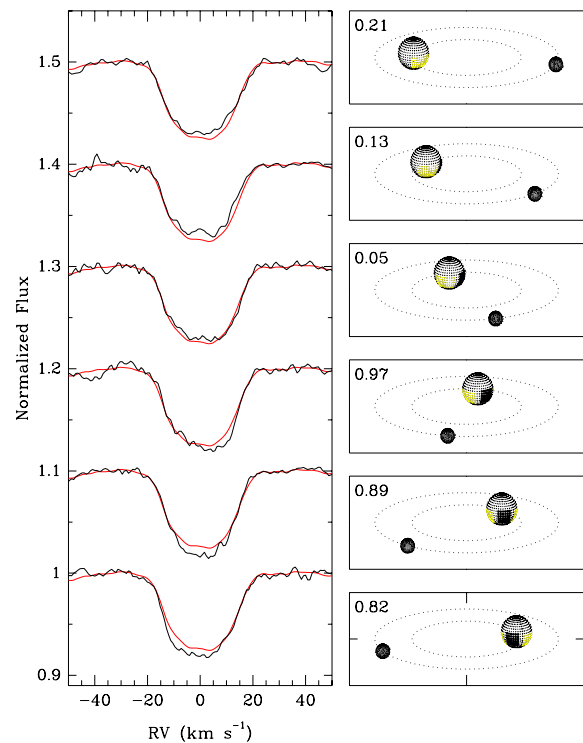
Figure 2. In the left-hand panel, we present the variability of Mn II line profiles in the spectra of the HgMn primary at six orbital phases. For comparison, for each phase the average of the five selected Mn II lines is overplotted with the same profile averaged over all phases (red line). In the right-hand panel, the position of the surface region with the Mn concentration is schematically indicated in dark colour. The yellow colour corresponds to regions with lower Mn abundance.

Mn II spectral lines (λλ4292, 4326, 4478, 4755, 4764) for the variability analysis. In most phases of our HARPS spectra, these appear free of blending with lines of the secondary star. In the left-hand panel of Fig. 2, we show for each phase the average of the five selected Mn II lines overplotted for comparison with the same profile averaged over all phases. In the right-hand panel of Fig. 2, we illustrate for each phase the corresponding binary configuration together with the expected location of the regions with Mn concentration. The region of the stellar surface facing permanently the secondary has a relatively low Mn abundance. A relative element underabundance on the side facing the companion was reported for the first time in the study of the AR Aur system with an HgMn primary by Hubrig et al. (2006). Interestingly, our study of the variability of Mn II line profiles in the primary of HD 161701 indicates that the surface region with the Mn concentration is not centred on the side pointing away from the companion, but rather on an intermediate longitude between the region facing the companion and the face of the preceding side. The spectral variability of the Ap component discovered by González et al. (2014) and the schematical distribution of enhanced elements on the surface of both components is displayed in Fig. 3. On the surface of this component, the region of the enhanced Ti and REE is permanently facing the primary while Fe is concentrated on the side hidden to the primary.

For magnetic field measurements, we applied two methods: the multiline Singular Value Decomposition (SVD) method for Stokes Profile Reconstruction introduced by Carroll et al. (2012) and the moment technique developed by Mathys (e.g. Mathys 1993). The basic idea of SVD is similar to the principal component analysis
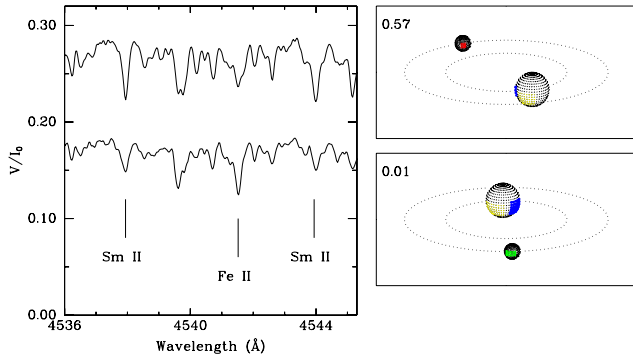
Figure 3. The left-hand panel shows variations of line profiles in the spectra of the Ap component belonging to the REE Sm and Fe at orbital phases 0.01 (bottom) and 0.57 (top) (González et al. 2014). In the right-hand panel, we schematically present the position of abundance spots on the surface of both, the Ap and HgMn components in the system HD 161701 at the same orbital phases. A chemical spot pattern with Ti and REEs on the surface of the Ap component permanently facing the primary is indicated in red, while Fe concentrated on the far side is indicated in green. For the HgMn primary star, the concentration of Mn and Cr elements is indicated in dark blue. Regions with lower Mn and Cr abundances are indicated in yellow.
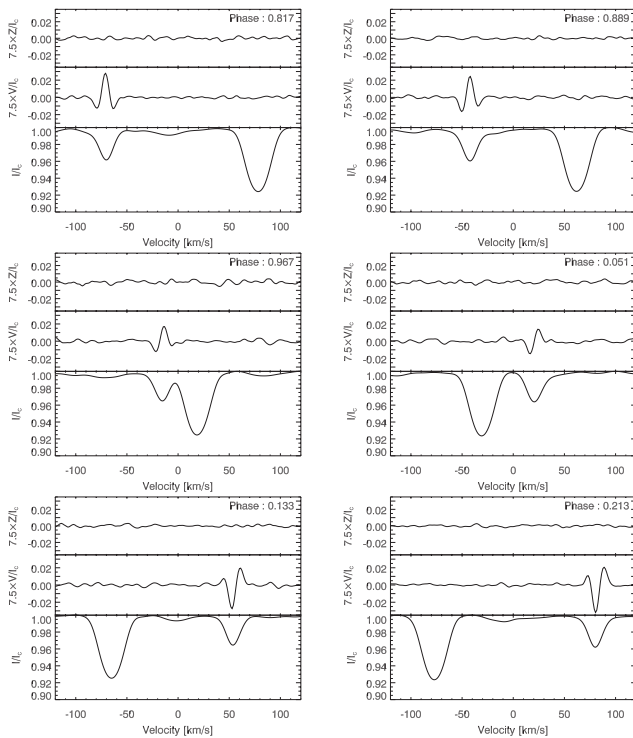

Figure 4. SVD Stokes *I*, *V*, and diagnostic null *Z* profiles obtained over six consecutive nights using 206 Fe II and Fe I lines. The *V* and *Z* profiles have been expanded by a factor of 7.5 and shifted upwards. No polarization is observed at the position of the average profile of the primary.

approach, where the similarity of the individual Stokes *V* profiles allows one to describe the most coherent and systematic features present in all spectral line profiles as a projection on to a small number of eigenprofiles (e.g. Carroll et al. 2009). The results obtained using the SVD method are presented in Fig. 4.

Distinct variable Stokes *V* Zeeman features are detected in the spectra of the Ap component while no Zeeman feature is detected in the HgMn primary. For the measurements of the magnetic field
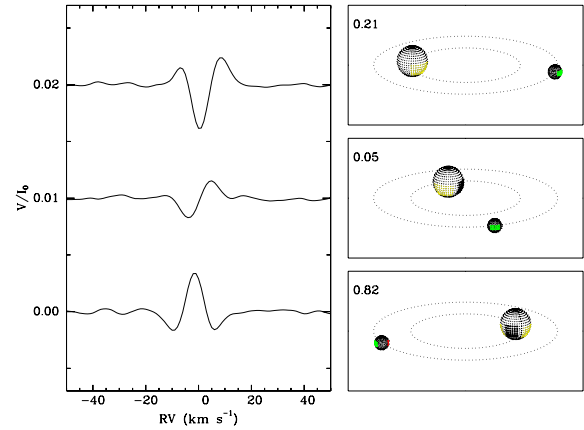

Figure 5. In the left-hand panel, we present the SVD Stokes *V* profiles corresponding to the orbital phases close to both quadratures (phases 0.82 and 0.21) and to the phase close to the time of the superior conjunction (phase 0.05). In the right-hand panel, we schematically present at the same phases the position of the Ap component relative to the primary component.

in the secondary, a line mask consisting of 206 Fe II and Fe I lines was created based on the line identification presented in the work of González et al. (2014). To illustrate the behaviour of the magnetic field in the Ap component over the orbital period, we present in Fig. 5 the SVD Stokes *V* profiles corresponding to the orbital phases close to both quadratures (phases 0.82 and 0.21) and to the phase close to the time of the superior conjunction (phase 0.05). The crossover profile at the orbital phase 0.82 indicates that both negative and positive magnetic poles are visible. In this phase, the longitudinal magnetic field changes the polarity from positive to negative (so-called negative crossover). Our spectropolarimetric observations do not cover the phases where we see the surface of the Ap star facing the primary component. Still, a reasonable conclusion is that the field on the surface permanently facing the primary component is positive and that it is negative on the far side. At the time of conjunction (phase 0.05), when the surface of the Ap component hidden to the primary becomes best visible, the field appears purely longitudinal of negative polarity. At the phase 0.21, the surface facing the primary component with the positive magnetic field becomes visible again and the observed Zeeman feature displays positive crossover. Such a behaviour of the longitudinal magnetic field is expected for the predominantly dipolar topology of the magnetic field. The quantitative results of the magnetic field measurements using the first-moment method implemented by Donati et al. (1997) are presented in the second column of Table 2, followed by the achieved S/N in column 3.

Due to the strong impact of blending by the line-rich spectra of the secondary, special care was taken to create a line list for the magnetic field measurements in the primary. The SVD analysis of 64 Fe II lines selected in the spectra of the primary and not strongly affected by blends shows no signal for the longitudinal magnetic field, with error bars between 52 G in the phase 0.82 up to 93 G in the phase 0.97. As an example of the impact of the noise level, we present in Fig. 6 the SVD profiles obtained for the phase 0.05 together with a simulated Zeeman feature corresponding to the detection limit of 79 G in the Stokes *V* profile.

The second method for the measurements, the moment technique, allows us not only to determine the mean longitudinal magnetic field, but also to prove the presence of the crossover effect and quadratic magnetic fields to constrain the magnetic field topology in more detail than can be done with the SVD method alone. The
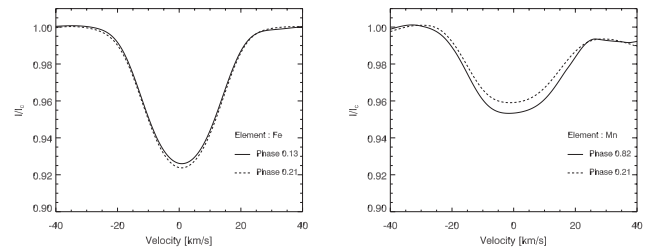
Table 2. Magnetic field measurements using the SVD method and the moment technique.

ϕ	$\langle B_z \rangle_{B, SVD}$ (G)	S/N_{SVD}	$\langle B_z \rangle_A$ (G)	$\langle B_z \rangle_B$ (G)	$\langle B_z \rangle_{A, Z}$ (G)	$\langle B_z \rangle_{B, Z}$ (G)	$\langle B_{xover} \rangle_A$ (G)	$\langle B_{xover} \rangle_B$ (G)	$\langle B_q \rangle_A$ (G)	$\langle B_q \rangle_B$ (G)
0.82	17 ± 10	1680	-6 ± 20	64 ± 51	5 ± 21	3 ± 48	118 ± 201	710 ± 201	1371 ± 1564	3115 ± 614
0.89	-92 ± 19	1620	-50 ± 22	-102 ± 46	-15 ± 23	-23 ± 45	308 ± 163	1152 ± 292	2115 ± 1287	2618 ± 1638
0.97	-108 ± 26	1400	-64 ± 23	-217 ± 47	-10 ± 24	-39 ± 46	84 ± 219	882 ± 302	2033 ± 872	2619 ± 723
0.05	-179 ± 29	1400	-71 ± 23	-226 ± 47	-16 ± 24	-39 ± 47	251 ± 225	234 ± 364	2148 ± 1044	3196 ± 865
0.13	-194 ± 29	1460	-34 ± 21	-166 ± 41	-14 ± 22	-34 ± 42	-87 ± 198	-888 ± 385	2266 ± 901	3504 ± 906
0.21	-130 ± 25	1570	-13 ± 22	-56 ± 36	9 ± 22	15 ± 35	-62 ± 173	-771 ± 227	2684 ± 993	3188 ± 994
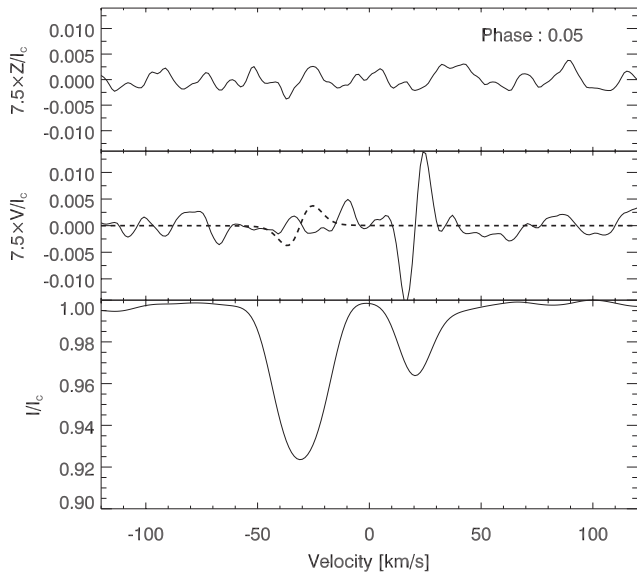
Figure 6. SVD Stokes *I*, *V*, and diagnostic null *Z* profiles for the primary component obtained at the phase 0.05 using 64 Fe II lines together with the simulated Zeeman feature (dashed line) corresponding to the detection limit of 79 G in the Stokes *V* profile.

Figure 7. The SVD profiles for the primary component. *Left:* calculated for 64 Fe II lines. *Right:* calculated for 14 Mn II lines. The maximum intensity of the Fe lines occurs at the phase 0.21, whereas lines of Mn show a maximum intensity at the phase 0.81.

measurements have been carried out on composite spectra, since spectral disentangling is not reliable for variable components without any modelling of the spectral variability to properly subtract the lines at each position. The results of the analysis for both components using the list of 64 Fe II lines, the measurements of the mean longitudinal magnetic field $\langle B_z \rangle$, the diagnostic null spectra $\langle B_z \rangle_Z$, crossover $\langle B_{xover} \rangle$, and quadratic magnetic field $\langle B_q \rangle$ in both components are presented in Table 2 in columns 4 to 11. For each measured line, the mean errors were derived through application of the formula for error propagation, taking into account the S/N of the spectra and the uncertainty of the wavelength calibration (Mathys 1994). We note that Fe lines in the spectra of the primary also appear variable, but at lower level compared to the variability of the Mn II lines. The SVD profiles presented in Fig. 7 and calculated for 64 Fe II and 14 Mn II lines illustrate, in addition, that the distribution of Mn and Fe on the surface of the primary are not identical, with the maximum intensity of Fe lines at the phase 0.21, whereas lines of Mn show maximum intensity at the phase 0.81.

As is shown in Table 2, the mean longitudinal magnetic field in the primary component of HgMn peculiarity, if indeed present, is variable and rather weak, only up to -70 G. A mean longitudinal magnetic field is detected at a 3σ significance level only in phase $\phi = 0.05$. The measurements of the magnetic field in the Ap component are mostly in good agreement with the SVD method, showing a longitudinal magnetic field of up to $\sim$200 G and a significant

crossover effect field at three orbital phases. The differences in the longitudinal magnetic field measurements between the SVD and the moment technique methods can be accounted to the line list selection. The crossover effect is undetected in the primary component. Similar results have been achieved for the measurements of the quadratic field: no quadratic field at a significance level of 3σ is detected in the primary, while it is detected in the secondary at five orbital phases.

4 DISCUSSION

The spectropolarimetric study of the system HD 161701 allowed us for the first time to get a deeper insight into the impact of binarity on the structure of magnetic fields on the surface of companions of different type of peculiarity. Using the SVD method, we do not detect any Zeeman feature in the Stokes *V* spectra at the position of the primary HgMn component. Using the moment technique, we detect a weak negative longitudinal magnetic field $\langle B_z \rangle = -71 \pm 23$ G at about 3σ level at the phase 0.05. We admit that due to the strong variable blending in the spectra of the primary by the lines of the secondary, such a detection can hardly be claimed as real without the future involvement of much better quality HARPS spectra. The difficulty to reliably measure the magnetic field in the HgMn primary component is explained in Fig. 8. In the left-hand panel, we display the disentangled left- and right-hand circularly polarized HARPS spectra in the vicinity of the marginally blended Mn II 4755 line using the method of González & Levato (2006). In the right-hand panel, we present the composite spectra in the same spectral region together with overimposed average disentangled spectra of the primary and the secondary. In the left-hand panel, the line profiles appear slightly different in differently polarized light, indicating the possible presence of a magnetic field. However, the appearance of the composite spectra suggests that a small contribution to the line profiles by the spectral lines of the secondary can still take place in the disentangled profiles.
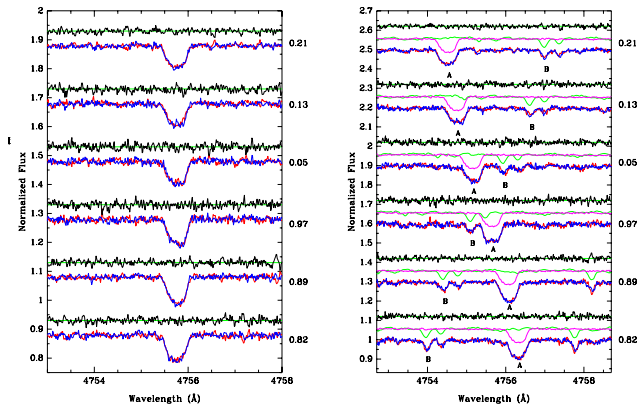
Figure 8. *Left:* disentangled left- and right-hand circularly polarized HARPS spectra (blue and red lines) in the vicinity of the marginally blended Mn II 4755 line. The black line shows the difference between the spectra obtained in opposite polarizations, while the green line corresponds to zero difference. *Right:* composite spectra together with overimposed average disentangled spectra of the primary (cyan line) and the secondary (green line).

Apart from HD 161701, only one other close binary system with a magnetic Ap component, the system HD 98088 with a lower mass Am companion, is currently known (e.g. Babcock 1958; Abt et al. 1968). The Ap component in HD 98088 exhibits a primary intensity maximum of the REE element europium at the surface persistently facing the companion, similar to the behaviour found in the Ap component in HD 161701. The detected spectrum variations take place with the same period as the orbital motion (Abt et al. 1968). According to Babcock (1958) and Folsom et al. (2013), also the longitudinal magnetic field varies with the same period and, similar to the magnetic field behaviour in the secondary of the HD 161701 system, the surface of the Ap component in HD 98088 facing the companion carries a positive magnetic field. The alignment of the magnetic axis with the orbital radius vector may indicate that the generation of the magnetic field was a dynamic process during the tidal synchronization. A magnetic instability was proposed by Arlt & Rüdiger (2011) and Szklarski & Arlt (2013) to generate Ap star fields. Tidal forces may alter the flows during the unstable phase as to align the final field geometries in the observed way. Regarding the inhomogeneous element distribution on the surface of the Ap component, it is possible that it predominantly depends on the magnetic field configuration. The distribution of different elements have previously been recognized to show symmetry relative to the topology of the magnetic field in Ap stars. In particular, REE spots have been found close to magnetic poles, while Fe has been depleted where REEs are overabundant (Ryabchikova 2003; Lüftinger et al. 2010). Clearly, further systematic searches for magnetic fields and spectral variability in similar binary systems should be conducted to properly evaluate theoretical models of the origin of magnetic fields and the development of chemical peculiarities.

REFERENCES

Abt H. A., Conti P. S., Deutsch A. J., Wallerstein G., 1968, ApJ, 153, 177
Arlt R., Rüdiger G., 2011, MNRAS, 412, 107
Babcock H. W., 1958, ApJS, 3, 141
Carroll T. A., Kopf M., Strassmeier K. G., Ilyin I., 2009, in Strassmeier K. G., Kosovichev A. G., Beckmann J., eds, Proc. IAU Symp. 259, Zeeman-Doppler imaging: Old Problems and New Methods. Cambridge Univ. Press, Cambridge, p. 633
Carroll T. A., Strassmeier K. G., Rice J. B., Künstler A., 2012, A&A, 548, A95
Donati J.-F., Semel M., Carter B. D., Rees D. E., Collier C. A., 1997, MNRAS, 291, 658
Folsom C. P., Likuski K., Wade G. A., Kochukhov O., Alecian E., Shulyak D., 2013, MNRAS, 431, 1513
González J. F., Levato H., 2006, A&A, 448, 283
González J. F. et al., 2014, A&A, 561, A63
Hubrig S., González J. F., Savanov I., Schöller M., Ageorges N., Cowley C. R., Wolff B., 2006, MNRAS, 371, 1953
Hubrig S., Ilyin I., Schöller M., Lo Curto G., 2013, Astron. Nachr., 334, 1093
Lüftinger T., Kochukhov O., Ryabchikova T., Piskunov N., Weiss W. W., Ilyin I., 2010, A&A, 509, A71
Mathys G., 1993, in Dworetsky M. M., Castelli F., Faraggiana R., eds, IAU Circ., 138, 232
Mathys G., 1994, A&AS, 108, 547
Ryabchikova T. A., 2003, in Balona L. A., Henrichs H. F., Medupe R., eds, ASP Conf. Ser. Vol. 305, Magnetic Fields in O, B and A Stars: Origin and Connection to Pulsation, Rotation and Mass Loss. Astron. Soc. Pac., San Francisco, p. 181
Szklarski J., Arlt R., 2013, A&A, 550, A94

This paper has been typeset from a TEX/LATEX file prepared by the author.